Detection and quantification of microplastics in various types of human tumor tissues

Jun Zhao [a,b], Haibo Zhang [a], Lei Shi [a], Yongshi Jia [a], Hailong Sheng [a,*]

[a] Cancer Center, Department of Radiation Oncology, Zhejiang Provincial People's Hospital (Affiliated People's Hospital), Hangzhou Medical College, Hangzhou, Zhejiang, China
[b] Reproductive Center, The Second Affiliated Hospital of Zhejiang Chinese Medical University, Hangzhou, Zhejiang, China

ARTICLE INFO

ABSTRACT

Microplastics (MPs) have been detected in various human tissues. However, whether MPs can accumulate within tumors and how they affect the tumor immune microenvironment (TIME) and therapeutic responses remains unclear. This study aimed to determine the presence of MPs in tumors and their potential effects on the TIME. Sixty-one tumor samples were collected for analysis. The presence of MPs in tumors was qualitatively and quantitatively assessed using pyrolysis-gas chromatography-mass spectrometry. MPs were detected in 26 of the samples examined. Three types of MPs were identified: polystyrene, polyvinyl chloride, and polyethylene. In lung, gastric, colorectal, and cervical tumors, the MP detection rates were 80 %, 40 %, 50 %, and 17 % (7.1–545.9 ng/g), respectively. MPs were detected in 70 % of pancreatic tumors (18.4–427.1 ng/g) but not detected in esophageal tumors. In pancreatic cancer, the MP-infiltrated TIME exhibited a reduction in CD8$^+$ T, natural killer, and dendritic cell counts, accompanied by substantial neutrophil infiltration. This study illustrates the potential presence of MPs in diverse tumors; varying adhesive affinities were observed among different tumor types. MPs may lead to a more adverse TIME in pancreatic tumors. Further investigations are warranted to assess whether MPs promote tumor progression and affect the efficacy of immunotherapy

1. INTRODUCTION

Globally, more than 330 million tons of plastic are produced annually. A considerable production increase was observed during the coronavirus disease 2019 because of the substantial manufacturing of plastic products (Zeb et al., 2024). However, less than 35 % of plastic waste is recycled, resulting in its disposal into the natural environment, which poses a considerable ecological threat. Microplastics (MPs), defined as particles with sizes below 5 mm, particularly micro- and nanosized plastic particles, originate from the continuous breakdown of plastic waste, which results in a reduced particle size (Osman et al., 2023). MPs have been detected in various waterbodies, soil, air, marine organisms, fruits, and vegetables (Nunes et al., 2023; van Raamsdonk et al., 2020; Zhang et al., 2020). Humans are continuously exposed to MPs via respiration, drinking water, and dietary consumption (Rahman et al., 2021). Recently, MPs have been identified in various human

matrices and organs including the gastrointestinal tract, respiratory tract, bloodstream, cardiac tissues, placenta, urine, and sperms (Horvatits et al., 2022; Jenner et al., 2022; Leslie et al., 2022; Marfella et al., 2024; Montano et al., 2023; Ragusa et al., 2022, 2021; Yang et al., 2023b).

According to the World Health Organization, one-fifth of the global population is expected to experience cancer during their lifetime. Tumors with a poor prognosis impose a substantial burden on the global population (Rumgay et al., 2022). Immunotherapy has gained momentum as a foundational approach for the treatment of various cancers. Consequently, the tumor immune microenvironment (TIME) is an important factor affecting the efficacy of immunotherapies against tumors (Mellman et al., 2023). The TIME refers to the complex local immune microenvironment comprising various immune cells, cytokines, extracellular matrix elements, and other factors, contributing to the intricate interplay between tumor cells and the immune system. The

TIME can markedly influence immune surveillance, immune evasion, and the effectiveness of immunotherapy. Under certain conditions, a multitude of factors can prompt the transition of the TIME into a suppressive one, thereby paradoxically favoring tumor cell survival and proliferation (Donne and Lujambio, 2023; Huang et al., 2021; Sheng et al., 2020). These alterations may lead to immunotherapy resistance. In contrast to the normal organ environments, the immune balance in the TIME is notably delicate, and the presence of MPs can undoubtedly trigger a complex and far-reaching array of effects on the TIME.

Within the TIME, MPs are perceived as foreign agents by the host immune system and can directly trigger localized immune responses (Kozlov, 2024). MPs are found to be directly phagocytosed by various immune cells, including macrophages and dendritic cells (DCs). This process interferes with regular metabolic activities, resulting in impaired antigen presentation and a reduced ability to eliminate other pathogens (van den Berg et al., 2022; Wolff et al., 2023). In addition, MPs can indirectly influence the immune microenvironment by promoting the secretion of diverse cytokines, including interleukin (IL)-1β, IL6, TNF-a, and IL-10 (Hamza et al., 2023; Ijaz et al., 2024; Rizwan et al., 2023). Murine models indicated that nanosized MPs induce lysosomal damage, resulting in the secretion of IL-1β by colonic macrophages. This induction prompts the differentiation of regulatory T and Th17 cells associated with T-cell exhaustion, thus establishing an immune environment favorable for the initiation and progression of colonic tumors (Yang et al., 2023a). MPs can adsorb various toxic substances, such as perfluoroalkyls and polyfluoroalkyls (Hatinoglu et al., 2023). The effects of these chemical substances on the TIME cannot be disregarded. Accordingly, MPs potentially disrupt the immune balance in the TIME.

In this study, we aimed to examine the presence of MPs in tumors and determine their potential effects on the TIME. To the best of our knowledge, this is the first study to identify MPs in human tumors including gastric, colorectal, lung, cervical, and pancreatic cancers. MPs can potentially disrupt or even reshape the TIME, resulting in a series of consequences that must be determined to establish their effects on tumor progression and immunotherapy efficacy.

2. Materials and methods

2.1. Participants

This study was approved by the Ethics Committee of Nanfang Hospital, Southern Medical University (No: NFEC-202110-K9), and fully complied with ethical principles, including The Code of Ethics of the World Medical Association (Declaration of Helsinki). Inclusion criteria were as follows: patients aged between 18 and 75 years and diagnosed pathologically with one of the following malignant tumors: lung cancer, cervical cancer, gastric cancer, colorectal cancer, esophageal cancer, or pancreatic cancer. Patients who had undergone surgery at Nanfang Hospital between January 2022 and January 2024 and provided written informed consent for the experiments conducted on their samples prior to surgery were enrolled. Exclusion criteria were as follows: patients did not undergo treatments such as arterial embolization. This preventive exclusion was implemented because arterial embolization carries the potential risk of contaminating tumor tissues with MPs. Surgical samples were collected from 61 patients, including 10 patients with lung cancer, 10 with gastric cancer, 10 with pancreatic cancer, 10 with colorectal cancer, 12 with cervical cancer, and 9 with esophageal cancer.

2.2. Materials

Deionized water was procured from the Clinical Medical Research Center of the Southern Hospital. Prior to utilization, the water was filtered through 1.6-μm glass fiber filters purchased from Whatman GF/A (1820–047; Maidstone, UK). Borosilicate glass bottles, syringes, and dishes were purchased from Zhuo-Sheng Biotechnology (Guangzhou, China). Potassium hydroxide (KOH) powder was obtained from Sigma-Aldrich (1310–58–3; St.Louis, MO, USA).

2.3. Quality control

Quality control was performed during all experiments. All glass and metal instruments were rinsed with deionized water, which was filtered through a 1.6 μm pore size glass fiber filter before use. A 10 % KOH solution was passed through the glass fiber filter. To avoid MPs pollution, cotton lab coats and latex gloves were used during the experimental procedures; all experiments were conducted under a laminar flow hood. Tumor samples obtained through surgical procedures were excised using a metallic instrument. As a control, three empty glass bottles were placed in the surgical room to simulate the tissue collection process. These glass bottles were subsequently subjected to the same procedure without the tumor tissue and then analyzed using pyrolysis–gas chromatography-mass spectrometry (Py-GCMS) for quality control purposes and to detect potential MPs contamination (Supplementary Figure 1).

2.4. Sample collection

Tumor tissues were placed in stainless-steel trays after excision. A portion of the tumor tissue was cut using a surgical blade and sufficient tissue was preserved for subsequent pathological examination. The weights of the excised tumor tissues are listed in Supplementary Tables 1–6. The collection personnel opened the glass bottles, promptly used stainless-steel forceps to transfer the samples into glass bottles, immediately closed the bottle caps, and surface-labeled the glass bottles. The tumor tissue specimens collected from 10 patients with pancreatic cancer were divided into two portions, in addition to preserving sufficient samples for pathological examination. One portion was allocated for pyrolysis–gas chromatography mass spectrometry (Py-GCMS) analysis and the other one was designated for cytometry using time-of-flight (CyTOF) analysis. All samples were collected using standardized surgical procedures and the patients did not incur any additional harm.

2.5. Sample processing

Tumor samples were placed in glass containers, marked with digital codes, and stored at −20 °C. The samples were digested at the Laboratory of the Clinical Research Center of the Southern Medical University. Cotton lab coats and latex gloves were used during experimental procedures to prevent MP pollution. Prior to initiating the experiments, all instruments, including stainless-steel scissors, forceps, and glassware, were thoroughly cleansed using 1.6 μm-filtered deionized water. Samples were processed in a laminar flow hood. The samples were then weighed and placed in glass containers. A 10 % KOH solution was prepared using 1.6 μm-filtered deionized water and KOH powder. The KOH solution and each sample were added to a glass bottle in a 20:1 ratio, sealed, and stored at 20 °C for 14 days. Subsequently, the specimens were filtered through a 1.6-μm glass fiber filter. The filter paper was then placed in 1.6-μm-filtered deionized water and washed (which flushes the material on the filter paper into the deionized water). The washings were then dried at room temperature and stored in glass Petri dishes. Three blank glass bottles collected from the operating room were processed and inspected using the same procedure.

2.6. Analysis of MPs by Py-GCMS

Filtered deionized water was added to a glass storage container containing a sample, followed by thorough mixing by repeated aspiration and expulsion using a glass pipette. The homogenized sample was then carefully withdrawn from the glass dish using a glass pipette and transferred to a Py-GCMS sampling crucible. The sample was placed into the Py-GCMS sampling crucible. The solvent used was 1.6 μm-filtered deionized water. The solvent was completely volatilized and tested

using Py-GCMS. The test cracking temperature was 550°C, and the split ratio was 5:1. Helium was used as the carrier gas. The chromatographic column used was Rtx-5MS (30 m × 0·25 mm × 0·25 μm). The heating program was 40°C for 2 min, followed by up to 320°C at a rate of 20 °C/ min and maintained for 14 min; the total program time was 30 min. The ion source temperature was 230°C, and the *m/z* scan range was 40–600. GC-MS model: GCMS-QP2020 Shimadzu; Cracker: PY-3030D Frontier. Py-GCMS can only detect nine types of MPs: polystyrene (PS), polyethylene (PE), polypropylene (PP), polymethyl methacrylate (PMMA), polyvinyl chloride (PVC), polyethylene terephthalate (PET), polycarbonate (PC), nylon 6 (PA6), and nylon 66 (PA66).

2.7. Limits of detection (LOD) and quantification (LOQ)

The LOD was calculated to be three times the standard deviation of the average long-term value of the blank signal. Values below the LOD were considered undetectable. The LOQ was set at three times the LOD. We utilized values greater than the detection LOQ to assess the MPs content in tumors. The LOD values for PS, PVC, and PE were 0.02, 0.02, and 0.5 ug/g, respectively.

2.8. CyTOF analysis

As stated earlier, we divided the 10 pancreatic tumor tissue samples into two parts: one part was subjected to Py-GC-MS analysis and the other part was allocated for subsequent CyTOF analysis. Tissues were digested using a solution of 1 mg/mL collagenase P (1 mM, COLLP-RO, Roche, CH) in RPMI 1640 medium (R7388; Sigma-Aldrich, USA). Cell suspensions were obtained by filtering the digested tissue specimen through a 70-μm filter (258368; NEST). Cell viability was determined using a 0.25 μM 194Pt (1 mM) live/dead staining solution (34963; Thermo Scientific, USA). The cells were also subjected to extracellular staining, followed by overnight fixation and DNA staining (191/193Ir; Fluidigm) and intracellular staining was performed following the addition of 20 % EQ beads (Fluidigm). For the CyTOF analysis, we used antibodies procured from BD Biosciences, BioXcell, BioLegend, and eBioscience (Supplementary Table 7). Antibody labeling was performed using the MaxPAR Antibody Labeling Kit (Fluidigm, USA), which incorporates antibodies with specific metal tags. Data were collected using a Helios instrument (Fluidigm, USA).

The data were de-barcoded from the raw data using a doublet-filtering scheme with unique mass-tagged barcodes (Zunder et al., 2015). Each.fcs file was normalized using bead normalization (Finck et al., 2013). Preprocessing was performed using FlowJo to remove debris (191Ir$^+$ 193Ir$^+$), dead cells (194Pt$^-$), and adherent cells. Individual, live, and intact cells were selected, followed by gating for CD45$^+$ immune cells for further analysis. The X-shift clustering algorithm was applied to categorize the cells into distinct phenotypes based on marker expression (Samusik et al., 2016). A dimensionality reduction algorithm, t-SNE, was employed for the two-dimensional visualization of high-dimensional data, revealing expression differences among different samples. Frequencies of annotated cell populations were statically analyzed using an unpaired two-tailed Student's t-test. CyTOF analysis was performed at the laboratory of Plttech Technology Company.

2.9. Statistical analysis

The Shapiro-Wilk test was used to determine whether data were normally distributed. An unpaired two-tailed Student's t-test was used to compare the TIME of two groups. Statistical significance was set to $P < 0.05$. All analyses were performed using GraphPad Prism 9.0 software (GraphPad Software, Inc., La Jolla, CA, USA).

3. Results

3.1. MPs concentrations in various human tumor tissues

Surgical specimens were collected from 61 patients with tumors who had not received other treatments (lung, n=10; cervical, n=12; gastric, n=10; colorectal, n=10; esophageal, n=9; pancreatic, n=10). The weight of collected tumor tissues ranged between 0.06 and 5.44 g (Supplementary Table 1–6). Tumor tissues were analyzed using Py-GCMS after appropriate processing.

Among the 61 tumor samples collected, MPs were identified in 26 samples (Fig. 1A). We simultaneously identified the types and quantities of MPs in 21 tumor tissues (mean ± standard deviation [SD]: 111.04 ± 156.77 ng/g). Three microplastic polymers were detected: PS, PVC, and PE. Multiple MPs were simultaneously detected in the most of the examined tumor samples (16/26). Among the 26 MPs-infiltrating tumor samples, a single microplastic type was detected in only 10 tumor tissues. Notably, PS emerged as the predominant MPs polymer type and was detected in 20 samples (59.56 ± 89.15 ng/g). PVC and PE were identified in 17 and 11 of the analyzed samples, respectively (PVC: 51.98 ± 81.61 ng/g; PE: 86.94 ± 116.84 ng/g) (Fig. 1B-D).

Herein, we collected specimens from six distinct tumor types: lung, cervical, gastric, esophageal, colorectal, and pancreatic. Among these, five types (lung, cervical, gastric, esophageal, and colorectal cancers) are known to possess direct communication channels with the external environment. Lung cancer exhibited the highest proportion of MPs, reaching 80 % (8/10), whereas the detection rates for cervical, gastric, and colorectal tumors were 17 % (2/12), 40 % (4/10), and 50 % (5/10), respectively. MPs were not detected in esophageal tumors (0/9). Notably, 70 % of the pancreatic cancer specimens (7/10) contained MPs. These results reveal differences in MP behavior across various types of malignancies (Fig. 2A-F).

Lung cancer specimens exhibit a high prevalence and diversity of MPs. Among the 10 lung cancer tissue samples, three contained all three types of MPs (i.e., PS, PVC, and PE), whereas three contained only PS and PE. The MPs levels were relatively high (122.30 ± 154.88 ng/g). Notably, substantial quantities of PS and PE were detected (PS: 41.10 ± 41.81 ng/g; PE: 79.28 ± 122.29 ng/g), respectively (Fig. 2A). Conversely, MPs detected in cervical cancer differed significantly, comprising low levels of only one type of microplastic (PE or PS, respectively) (Fig. 2B).

Considering digestive tract tumors, although gastric and colorectal cancers are considered to be highly exposed to MPs, the proportion and diversity of MPs in tumors were moderate. Among the four cases of gastric cancers with detected MPs, only one case exhibited all three types of MPs, whereas one case had two types and two cases had only one type each. All three types of MPs were detected in one case of colorectal cancer, while two cases had two types of MPs each, and two cases had only one type of MPs each. Unlike other tumors, gastric cancers were predominantly infiltrated by PVC, followed by PS and PE (PVC: 78.23 ± 109.23 ng/g; Fig. 2C-D). Despite the early contact of the esophagus with external food during the digestive process, MPs were not detected in any of the nine esophageal cancer samples (Fig. 2E).

Interestingly, the proportion of MPs detected in pancreatic cancer is second only to that detected in lung cancer. Pancreatic cancer exhibited a unique particle distribution, with PS (6/10) and PVC (6/10) identified as the predominant MPs (PS: 128.73 ± 138.45 ng/g; PVC: 29.98 ± 28.25 ng/g). Among these, PS exhibited the highest level, reaching 356 ng/g in one patient sample, representing the highest detected PS content among all tumors. Only one sample contained minimal amounts of PE (2.1 ng/g) (Fig. 2F). Fig. 3 illustrates the detection results for representative patients with lung, cervical, gastric, colorectal, and pancreatic cancers.
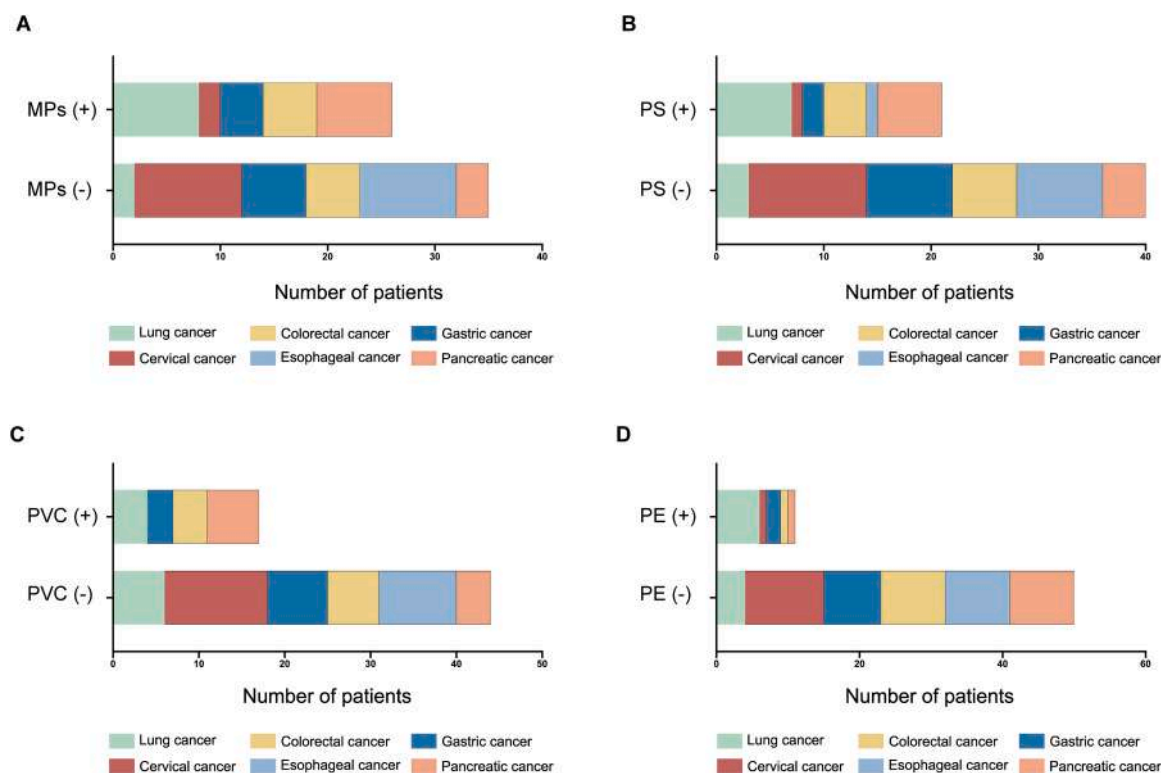
Fig. 1. Detection of microplastics in tumor samples. A: The number of samples with and without MPs detected in 61 tumor samples (lung, n=10; cervical, n=12; gastric, n=10; colorectal, n=10; esophageal, n=9; pancreatic, n=10). B-D: The number of samples with PS (B), PVC (C), and PE (D) detected in 61 tumor samples (n=61). All values are above the LOQ. LOQ, limit of quantitation; MPs, microplastics; PE, polyethylene; PS, polystyrene; PVC, polyvinyl chloride.

3.2. The impact of MPs on the TIME of pancreatic cancer

In the current study, we observed the presence of MPs in 70 % of pancreatic tumor samples (5/7), a proportion surpassed only by lung cancer and notably higher than that detected in other tumors. We divided the 10 pancreatic cancer samples into two portions, with one portion subjected to Py-GCMS and the other to CyTOF analysis. Based on the Py-GCMS results, we categorized these 10 patients into MPs (-) and MPs (+) groups. We analyzed the TIME of pancreatic cancer with and without MPs and detected notable differences between the two conditions (Fig. 4A). Specifically, compared with the TIME of MPs (-) pancreatic tumors, the TIME of MPs (+) pancreatic tumors was characterized by a significant reduction in known antitumor cytotoxic cells, including CD8$^+$ T cells ($P = 0.0023$) and natural killer cells (NK; $P = 0.0224$), as well as a significant reduction in dendritic cells ($P = 0.0052$). In addition, we detected a significant increase in the number of neutrophils in the MPs (+) tumors ($P = 0.0144$), whereas there were no significant differences with respect to the numbers of CD4$^+$ T cells, macrophages, B cells, or $\gamma\delta$T cells (Fig. 4B). These preliminary results suggest that MPs affect the TIME in pancreatic cancer.

4. Discussion

MPs are ubiquitous throughout ecosystems. Although MPs have been observed in various human organs, including the blood, lungs, heart, and placenta, their potential to accumulate in tumor tissues remains to be established (Horvatits et al., 2022; Leslie et al., 2022; Ragusa et al., 2021; Yang et al., 2023b). Tumors represent a significant global burden. Data from 2020 indicate that tumors are the second leading cause of death (Sung et al., 2021). In the current study, we demonstrated the presence of MPs in various human tumors. In addition, we identified the specific types and quantities of MPs in these tumors.

The distribution of MPs differs among the different organs. PS, PE,

PET, PP, and PMMA have been detected in the human blood (Leslie et al., 2022). PP is the predominant type of MPs identified in the placenta and lungs (Ragusa et al., 2021). Six types of MPs have been identified in the cirrhotic liver tissues, with PS and PVC showing the highest levels (Horvatits et al., 2022). In this study, we identified three types of MPs (PS, PVC, and PE) in six tumor types. Other MPs, such as PET or PP, were not detected. Multiple types of MPs were detected at relatively high levels in lung cancer samples. Cervical cancer tissues were infiltrated by a single type of microplastic at relatively low levels. No MPs was detected in the examined esophageal cancer specimens. Pancreatic cancer exhibited a distinctive MPs distribution, primarily comprising PS and PVC, with higher levels of PS. Similar to substantial differences in MPs observed in various human tissues in other studies, our results reveal that MPs accumulation varies markedly among different tumors.

In addition to the differences in MPs present in distinct tumor tissues, we identified notable differences between tumor and normal tissues. A previous study identified the presence of 12 types of MPs in 13 lung tissue samples, with PP (23 %) exhibiting the highest abundance (Jenner et al., 2022). Notably, normal lung tissues appear to display a greater variety of MPs than lung cancer tissues examined in our study, and PP, which was the most prevalent, was not detected in our lung cancer tissue specimens. The phenomenon may be influenced by the varying geographical locations of the patients and the background levels of MPs in the air; however, it is more likely that tumors and normal tissues exhibit different affinities for MPs. One possible mechanism is that certain molecules in tumors exhibit distinct affinities for various MPs. Studies have suggested that PS can selectively bind to the cell surface receptor T-cell membrane protein 4 (TIM-4), facilitating the entry of MPs into cells. High expression of TIM-4 in tumor tissues may contribute to the increased capture and internalization of PS (Kuroiwa et al., 2023). Kopatz et al. have shown that nanoparticles can enter the mouse brain within a few hours of ingestion and that nanoscale MPs can form a lipid
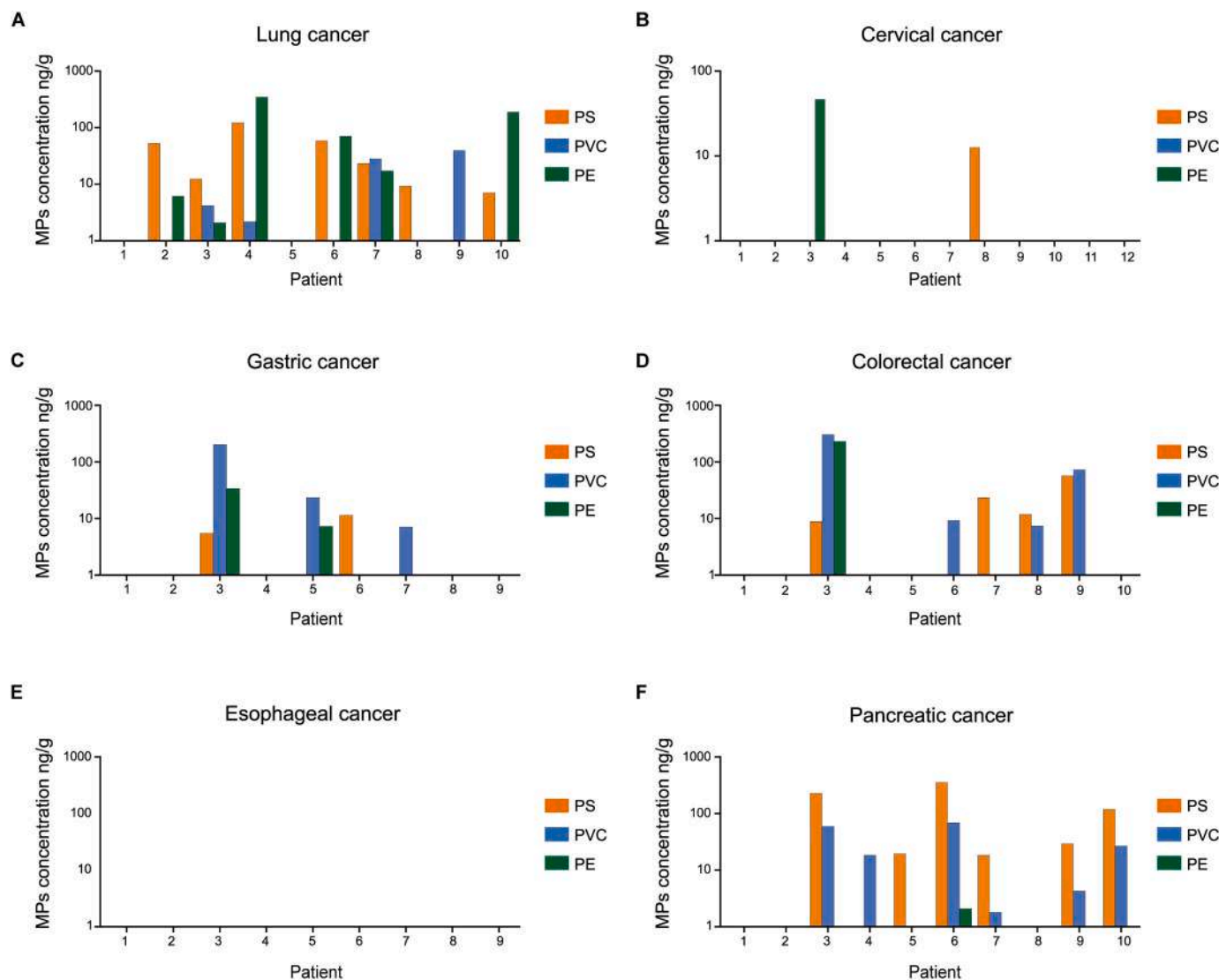
Fig. 2. Differences in the presence of MPs in different tumors. A-F: The types and levels of MPs detected in 61 tumor samples, including 10 lung cancers (A), 12 cervical cancers (B), 10 gastric cancers (C), 10 colorectal cancers (D), 9 esophageal cancers (E), and 10 pancreatic cancers (F). All values are above the LOQ. LOQ, limit of quantitation; MPs, microplastics; PE, polyethylene; PS, polystyrene; PVC, polyvinyl chloride.

layer by binding to specific lipids on the surface, enabling their penetration across the blood-brain barrier (Kopatz et al., 2023). MPs were found to exhibit a high affinity for binding to α-synuclein fibrils within neuronal cells, spontaneously forming a stable complex with over 100 α-synuclein monomers (Liu et al., 2023). Collectively, the findings of these studies suggest that MPs possess specific affinities for various biomolecules, allowing them to bind, transport, or localize to specific sites within the body. Another possibility is that different tumors may exhibit varying clearance efficiencies for different types of MPs, thereby resulting in distinct levels of MPs accumulation. However, both hypotheses require further validation. The current study lays the groundwork for constructing animal tumor models with MPs and delving deeper into the biological effects of MPs within tumors. We also observed substantial individual variations among patients with the same tumor type. These differences may be related to variations in gene expression in patients, environmental factors associated with residence, and dietary patterns.

Research on MPs accumulation in humans has predominantly focused on identifying the types of MPs. However, data on their actual quantities are lacking (Vethaak and Legler, 2021). This has also been the focal point of the ongoing debate on whether MPs pose a potential health risk to humans. It has been speculated that if MPs are found in human tissues, small amounts may be rapidly excreted through the body's natural clearance mechanisms, thereby preventing substantial harm (Prata et al., 2020). To address this issue, it is crucial to establish precise levels of MPs and determine their potential to accumulate in organs. In this study, we quantified MPs in tumors from various systems, including the respiratory, digestive, and reproductive systems, to determine the order of magnitude of MPs present in human tumors. Our research provides crucial groundwork for subsequent in vivo studies on the dose-dependent toxicity of MPs.

With the advent of the immunotherapy era, immunotherapy has become a crucial treatment modality for various cancers, including lung and colorectal cancer (Lahiri et al., 2023; Prakash et al., 2023). Notably, the effectiveness of immunotherapy is markedly dependent on the TIME. Any substance infiltrating the tumor microenvironment could influence the transition between cold and hot TIME (Mellman et al., 2023; Peng et al., 2022). The status may be disrupted in the presence of MPs. The MP-mediated induction of localized abnormal inflammation has previously been reported, with MPs being shown to disrupt the local testicular tissues of male rats by promoting the secretion of factors such as IL-6, nuclear factor κB, and IL-1β (Hamza et al., 2023; Ijaz et al., 2024;
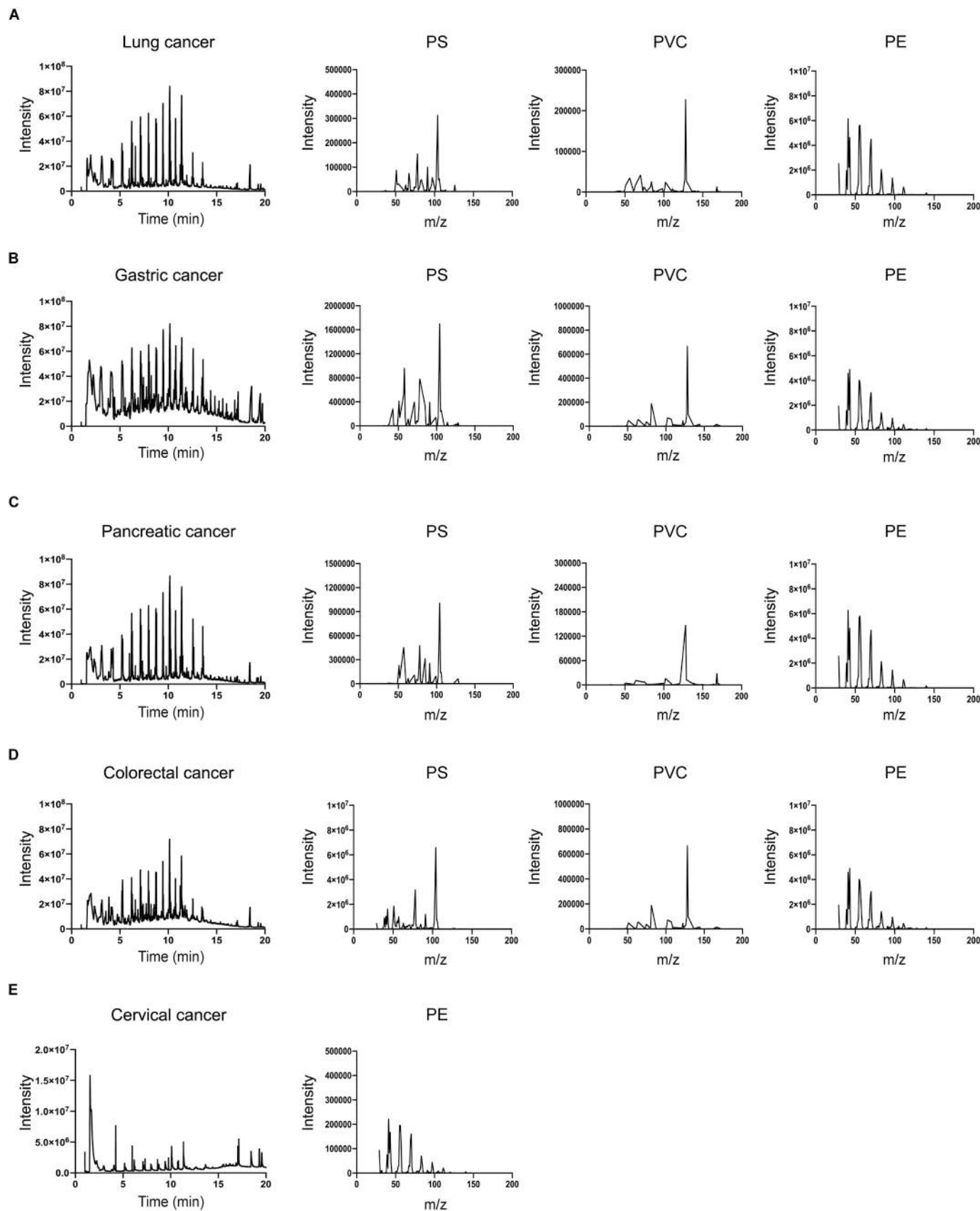
Fig. 3. Representative total ion chromatogram and mass spectra of patient samples. A-F: Representative total ion chromatogram and mass spectrum of MPs detected in patient samples using Py-GCMS. The samples include lung cancer (A), gastric cancer (B), pancreatic cancer (C), colorectal cancer (D), and cervical cancer specimens. All values are above the LOQ. LOQ, limit of quantitation; MPs, microplastics; Py-GCMS, pyrolysis–gas chromatography-mass spectrometry.
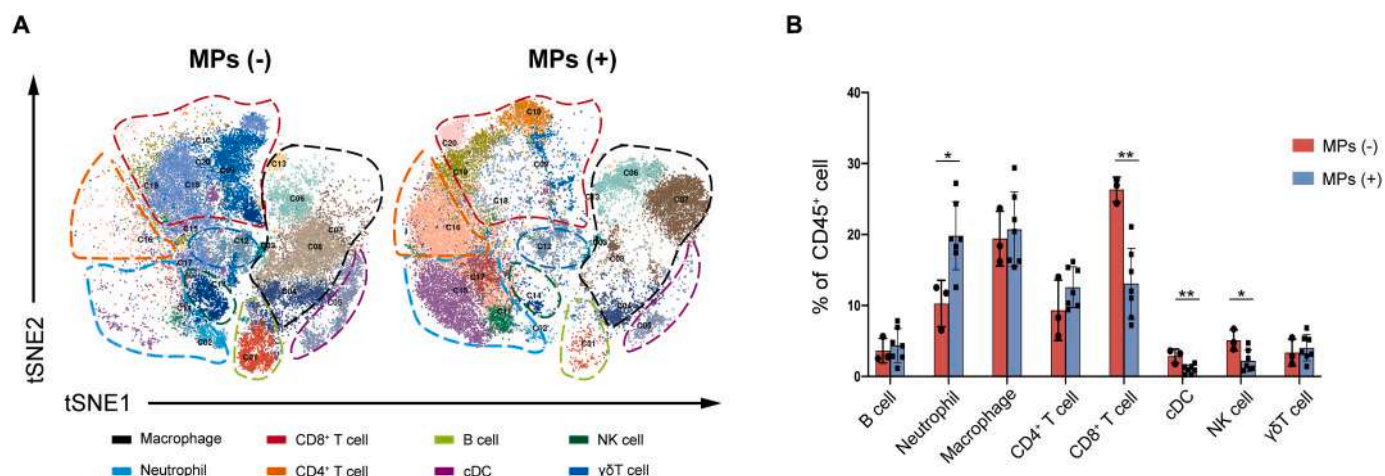
Fig. 4. The TIME of MPs (-) and MPs (+) pancreatic cancer. A: Representative mass cytometry flow plots of TIME in MPs (-) and MPs (+) pancreatic cancer. B: Comparative analysis of CD4$^+$, CD8$^+$, macrophages, B cells, DCs, NK cells, and γδT cells in MPs (-) and MPs (+) pancreatic cancer. n=3–7. Data values represent the mean ± standard deviation (SD). An unpaired two-tailed Student t-test was performed for statistical analysis. *$P < 0.05$. **$P < 0.01$. DCs, dendritic cells; MPs, microplastics; NK, natural killer; TIME, tumor immune microenvironment.

Wolff et al., 2023; Yin et al., 2023). Pancreatic cancer is widely recognized as a cold tumor with a poor prognosis, exhibiting a minimal response to immunotherapy (Bear et al., 2020). Despite extensive research on the etiology of pancreatic cancer as a cold tumor, many aspects remain elusive. Although disruption of the immune balance by MPs is well documented, their specific influence on the TIME of pancreatic cancer and their immunotherapeutic efficacy remains unknown (Liu et al., 2024; Xu et al., 2024). Our research results indicate an unusually high proportion of MPs detected in pancreatic cancer, with a wide variety of infiltrating MPs types. Furthermore, the preliminary analysis indicated a reduction in the number of cytotoxic cells, represented by CD8$^+$ and NK cells, in MPs-infiltrated pancreatic tumors. Immunotherapy heavily relies on CD8$^+$ and NK cells, emphasizing the potential effect of MPs on the effectiveness of immunotherapy in pancreatic cancer. The number of professional antigen-presenting cells, DCs, also decreased. This reduction may lead to impaired antigen presentation, thereby inhibiting CD8$^+$ cell activation. Additionally, we observed that the presence of MPs was associated with neutrophil accumulation in tumors. Neutrophils may play a role in worsening the TIME. Tumors can exploit neutrophils to inhibit the activity of immune cells, promoting tumor escape (Gungabeesoon et al., 2023; Hedrick and Malanchi, 2022). Therefore, neutrophil aggregation in MPs (+) pancreatic cancer may be one of the factors contributing to the deterioration of TIME. Our preliminary results suggest that MPs may be one of the factors contributing to the immunosuppressive microenvironment of pancreatic cancer, warranting further exploration.

In recent studies, the air in operating rooms has been examined and the presence of MPs was discovered (Field et al., 2022). This suggests that the MPs detected in surgical specimens may have been acquired upon contact with the air in the operating room. Furthermore, numerous pieces of equipment in the operating room are fabricated from plastic materials, including certain large instruments and intravenous bags used during the patient's surgery. However, these plastic products may not directly come into contact with tumor tissues. To eliminate the possibility of exogenous MPs contamination, we simulated the sample collection process in an operating room and collected three controls for simultaneous testing; MPs contamination was not detected in the controls.

The limitations of the current study need to be addressed. Previous studies have suggested that the effects and mechanisms of action of nanosized and microsized MPs on cells and tissues differ fundamentally (da Silva Brito et al., 2022). Although Py-GC-MS allows the qualitative and quantitative analyses of MPs, we were unable to analyze the size,

shape, and precise numbers of the MPs particles in tumor tissues owing to methodological limitations; this is consistent with the findings reported previously. Furthermore, Py-GC-MS only detects nine types of MPs, potentially overlooking other types of MPs present within the tumors. Secondly, the sample size was relatively small. However, to the best of our knowledge, this is the first report to establish preliminary evidence for the presence of MPs in tumors.

In summary, this study provides new insights into human exposure to MPs. Given the pivotal role of the immune microenvironment in tumor development and the efficacy of immunotherapy, the presence of exogenous and potentially harmful MPs in the TIME demands considerable attention. Further investigations are needed to determine whether the presence of MPs in tumors disrupts or reshapes the TIME, potentially accelerating tumor progression and resistance to treatment.

CRediT authorship contribution statement

Yongshi Jia: Writing – review & editing, Resources, Project administration, Formal analysis. **Lei Shi:** Writing – review & editing, Validation, Investigation, Funding acquisition. **Haibo Zhang:** Validation, Supervision, Resources, Conceptualization. **Jun Zhao:** Software, Methodology, Investigation, Formal analysis, Data curation. **Hailong Sheng:** Writing – review & editing, Writing – original draft, Visualization, Validation, Supervision, Software, Project administration, Methodology, Investigation, Funding acquisition, Formal analysis, Conceptualization.

Declaration of Competing Interest

The authors declare that they have no known competing financial interests or personal relationships that could have appeared to influence the work reported in this paper.

Data availability

Data will be made available on request.

Acknowledgements

Appendix A. Supporting information

Supplementary data associated with this article can be found in the online version at doi:10.1016/j.ecoenv.2024.116818.

References

Bear, A.S., et al., 2020. Challenges and opportunities for pancreatic cancer immunotherapy. Cancer Cell 38, 788–802.

van den Berg, A.E.T., et al., 2022. Environmentally weathered polystyrene particles induce phenotypical and functional maturation of human monocyte-derived dendritic cells. J. Immunotoxicol. 19, 125–133.

Donne, R., Lujambio, A., 2023. The liver cancer immune microenvironment: therapeutic implications for hepatocellular carcinoma. Hepatology 77, 1773–1796.

Field, D.T., et al., 2022. Microplastics in the surgical environment. Environ. Int 170, 107630.

Finck, R., et al., 2013. Normalization of mass cytometry data with bead standards. Cytom. A 83, 483–494.

Gungabeesoon, J., et al., 2023. A neutrophil response linked to tumor control in immunotherapy. Cell 186, 1448–1464 e20.

Hamza, A., et al., 2023. Rhamnetin alleviates polystyrene microplastics-induced testicular damage by restoring biochemical, steroidogenic, hormonal, apoptotic, inflammatory, spermatogenic and histological profile in male albino rats. Hum. Exp. Toxicol. 42, 9603271231173378.

Hatinoglu, M.D., et al., 2023. Modified linear solvation energy relationships for adsorption of perfluorocarboxylic acids by polystyrene microplastics. Sci. Total Environ. 860, 160524.

Hedrick, C.C., Malanchi, I., 2022. Neutrophils in cancer: heterogeneous and multifaceted. Nat. Rev. Immunol. 22, 173–187.

Horvatits, T., et al., 2022. Microplastics detected in cirrhotic liver tissue. EBioMedicine 82, 104147.

Huang, Y., et al., 2021. Wnt/beta-catenin inhibitor ICG-001 enhances the antitumor efficacy of radiotherapy by increasing radiation-induced DNA damage and improving tumor immune microenvironment in hepatocellular carcinoma. Radio. Oncol. 162, 34–44.

Ijaz, M.U., et al., 2024. Mitigative potential of kaempferide against polyethylene microplastics induced testicular damage by activating Nrf-2/Keap-1 pathway. Ecotoxicol. Environ. Saf. 269, 115746.

Jenner, L.C., et al., 2022. Detection of microplastics in human lung tissue using muFTIR spectroscopy. Sci. Total Environ. 831, 154907.

Kopatz, V., et al., 2023. Micro- and nanoplastics breach the blood-brain barrier (BBB): biomolecular corona's role revealed. Nanomater. (Basel) 13.

Kozlov, M., 2024. Landmark study links microplastics to serious health problems. Nature.

Kuroiwa, M., et al., 2023. Tim4, a macrophage receptor for apoptotic cells, binds polystyrene microplastics via aromatic-aromatic interactions. Sci. Total Environ. 875, 162586.

Lahiri, A., et al., 2023. Lung cancer immunotherapy: progress, pitfalls, and promises. Mol. Cancer 22, 40.

Leslie, H.A., et al., 2022. Discovery and quantification of plastic particle pollution in human blood. Environ. Int 163, 107199.

Liu, Z., et al., 2023. Anionic nanoplastic contaminants promote Parkinson's disease-associated alpha-synuclein aggregation. Sci. Adv. 9, eadi8716.

Liu, W., et al., 2024. Single-cell transcriptome analysis of liver immune microenvironment changes induced by microplastics in mice with non-alcoholic fatty liver. Sci. Total Environ. 912, 168308.

Marfella, R., et al., 2024. Microplastics and nanoplastics in atheromas and cardiovascular events. N. Engl. J. Med 390, 900–910.

Mellman, I., et al., 2023. The cancer-immunity cycle: indication, genotype, and immunotype. Immunity 56, 2188–2205.

Montano, L., et al., 2023. Raman Microspectroscopy evidence of microplastics in human semen. Sci. Total Environ. 901, 165922.

Nunes, B.Z., et al., 2023. Microplastic contamination in seawater across global marine protected areas boundaries. Environ. Pollut. 316, 120692.

Osman, A.I., et al., 2023. Microplastic sources, formation, toxicity and remediation: a review. Environ. Chem. Lett. 1–41.

Peng, S., et al., 2022. Tumor-microenvironment-responsive nanomedicine for enhanced cancer immunotherapy. Adv. Sci. (Weinh.) 9, e2103836.

Prakash, A., et al., 2023. Tumor-derived extracellular vesicles in the colorectal cancer immune environment and immunotherapy. Pharm. Ther. 241, 108332.

Prata, J.C., et al., 2020. Environmental exposure to microplastics: an overview on possible human health effects. Sci. Total Environ. 702, 134455.

van Raamsdonk, L.W.D., et al., 2020. Current insights into monitoring, bioaccumulation, and potential health effects of microplastics present in the food chain. Foods 9.

Ragusa, A., et al., 2021. Plasticenta: first evidence of microplastics in human placenta. Environ. Int 146, 106274.

Ragusa, A., et al., 2022. Raman microspectroscopy detection and characterisation of microplastics in human breastmilk. Polym. (Basel) 14.

Rahman, A., et al., 2021. Potential human health risks due to environmental exposure to nano- and microplastics and knowledge gaps: a scoping review. Sci. Total Environ. 757, 143872.

Rizwan, A., et al., 2023. Attenuative effect of astilbin on polystyrene microplastics induced testicular damage: Biochemical, spermatological and histopathological-based evidences. Toxicol. Appl. Pharm. 471, 116559.

Rumgay, H., et al., 2022. Global burden of primary liver cancer in 2020 and predictions to 2040. J. Hepatol. 77, 1598–1606.

Samusik, N., et al., 2016. Automated mapping of phenotype space with single-cell data. Nat. Methods 13 (6), 493.

Sheng, H., et al., 2020. ATR inhibitor AZD6738 enhances the antitumor activity of radiotherapy and immune checkpoint inhibitors by potentiating the tumor immune microenvironment in hepatocellular carcinoma. J. Immunother. Cancer 8.

da Silva Brito, W.A., et al., 2022. Consequences of nano and microplastic exposure in rodent models: the known and unknown. Part Fibre Toxicol. 19, 28.

Sung, H., et al., 2021. Global Cancer Statistics 2020: GLOBOCAN estimates of incidence and mortality worldwide for 36 cancers in 185 countries. CA Cancer J. Clin. 71, 209–249.

Vethaak, A.D., Legler, J., 2021. Microplastics and human health. Science 371, 672–674.

Wolff, C.M., et al., 2023. Immune and inflammatory responses of human macrophages, dendritic cells, and T-cells in presence of micro- and nanoplastic of different types and sizes. J. Hazard Mater. 459, 132194.

Xu, W., et al., 2024. Single-cell RNA-seq analysis decodes the kidney microenvironment induced by polystyrene microplastics in mice receiving a high-fat diet. J. Nanobiotechnology 22, 13.

Yang, Q., et al., 2023a. Nanoplastics shape adaptive anticancer immunity in the colon in Mice. Nano Lett. 23, 3516–3523.

Yang, Y., et al., 2023b. Detection of various microplastics in patients undergoing cardiac surgery. Environ. Sci. Technol. 57, 10911–10918.

Yin, K., et al., 2023. Polystyrene microplastics promote liver inflammation by inducing the formation of macrophages extracellular traps. J. Hazard Mater. 452, 131236.

Zeb, A., et al., 2024. Microplastic pollution in terrestrial ecosystems: global implications and sustainable solutions. J. Hazard Mater. 461, 132636.

Zhang, Q., et al., 2020. A review of microplastics in table salt, drinking water, and air: direct human exposure. Environ. Sci. Technol. 54, 3740–3751.

Zunder, E.R., et al., 2015. Palladium-based mass tag cell barcoding with a doublet-filtering scheme and single-cell deconvolution algorithm. Nat. Protoc. 10, 316–333.